Characterization of solid bitumen from Panandhro lignite (western India) based on FTIR and Pyrolysis GC-MS study

Runcie P. Mathews* and Bhagwan D. Singh

Organic Petrology Group, Birbal Sahni Institute of Palaeosciences, 53-University Road, Lucknow 226 007, India

In this study, FTIR and pyrolysis GC-MS analysis methods are used to characterize the handpicked solid bitumen (viscous residue of hydrocarbon) found as fillings in the lignite of Panandhro field, Gujarat. The FTIR data shows that solid bitumen is marked by intense aliphatic CH_x stretching peaks between 3000 and 2800 cm^{-1}, medium absorption of OH stretching, aromatic C=C, and aliphatic deformation peaks. A factor versus C factor plot indicates that it is mainly composed of type-II kerogen (organic matter). The pyrolysis GC-MS data shows the highly aliphatic nature of the solid bitumen. The overall characteristics indicate that the studied solid bitumen is of pre-oil generation type and formed from increase in thermal maturity of lignites.

Keywords: FTIR, Gujarat, Panandhro lignite, pyrolysis GC-MS, solid bitumen.

BITUMEN is that part of the organic matter that is soluble in organic solvents[1]. The solid bitumen is a viscous residue of hydrocarbon, amorphous in nature, and has asphaltic constituents. It is a secondary product of the coalification/maturation process, formed by various processes, such as maturity changes on subsequent burial (thermal alteration of organic materials), by thermal cracking of oil, by deasphalting of oil by gas, and by biodegradation. The solid bitumens are found in or are associated with organic rich sedimentary rocks that suffered advanced stages of thermal maturation[2]. They are the bitumen in mobile phase which gets solidified under surface conditions[3]. Although they are expelled hydrocarbons, their presence in sedimentary reservoir rocks causes a significant impact on the hydrocarbon potential. During petroleum exploration, the presence of solid bitumen can cause profound economic impact by changing the overall reservoir characteristics[4,5]. In vitrinite-poor sedimentary sequences, the presence of solid bitumen can be an indicator of oil/gas as well as maturity, and can also be used to get information on migration paths[6–8].

Solid bitumen is found in various petroliferous basins around the world, and has been extensively studied[2,5,9–12]. However, solid bitumen from Indian sedimentary basins has not been studied yet. Here, the geochemical charac-

terization has been done on solid bitumen collected from Panandhro lignite mine of the Kachchh Basin, Gujarat state, by fourier transform infrared (FTIR) spectroscopic method. The result is also compared with the FTIR data of solid bitumen collected from the Neyveli lignite mine of Cauvery Basin, Tamil Nadu. Further, pyrolysis-gas chromatography-mass spectrometry (Py–GC–MS) has been carried out on Panandhro solid bitumen to understand the nature of the origin. Lignite is considered as a source of hydrocarbons under certain specific conditions. Earlier studies show the ability of this sedimentary rock to produce unconventional oil/gas[13,14]. Further, the Kachchh Basin is considered as category-II (identified hydrocarbon prospectively) basin[15], with one oil and two gas strikes on exploration. The palaeocene sedimentary units are also quantified as one of the source rock of hydrocarbons. Although, the onshore sedimentary sequences with lignites and shales are not promising, the same sequences in the offshore region have good hydrocarbon prospects[16]. Therefore, characterization of solid bitumen from Panandhro will provide additional information to the hydrocarbon source characteristics of lignite-bearing Kachchh Basin.

The Kachchh Basin encloses one of the best developed and undisturbed Mesozoic–Cenozoic sequences in western India[17]. The basin is bounded by Nagar Parker uplift in the north and Kathiawar uplift (Saurashtra horst) in the south. The Radhanpur Arch hinterland high limits the basin towards the east, while it is open at the western side merging with the continental shelf. The basin has a general slope towards W–SW. Tertiary sediments occur on the western part of the basin with a significant amount occurring in the offshore region extending up to the present continental shelf. Lignite forms enormous thickness in the basin associated with Naredi Formation (Paleocene–Eocene)[17]. This lignite is presently mined from Panandhro and Matanomadh open cast mines by the Gujarat Mineral Development Corporation (GMDC) Ltd. the Panandhro lignite field (Figure 1), the second largest lignite mine in the country after Neyveli, extends over an area of 11.33 sq. km. The mine consists of two exploitable lignite seams–lower (~4 m thick) and upper (~23 m thick) separated by shale and clay beds. The generalized Cenozoic lithostratigraphic sequence of the Kachchh Basin is given in Figure 2.

Solid bitumen found as fillings in cracks of the Panandhro lignites was selected for our study. Samples for FTIR were prepared as potassium bromide (KBr) pellets following standard procedures[18]. The analyses were performed using a Nicolet instrument (MAGNA 500) operated by OMNIC software. Spectra were obtained for a defined area by co-adding up to 512 scans with a spectral resolution of 4 cm^{-1}. The recorded spectra ranged between 4000 cm^{-1} and 500 cm^{-1}. The band (peak) assignments were done based on published literature[18–21]. For py-GC-MS, the samples were pyrolysed at 550°C for

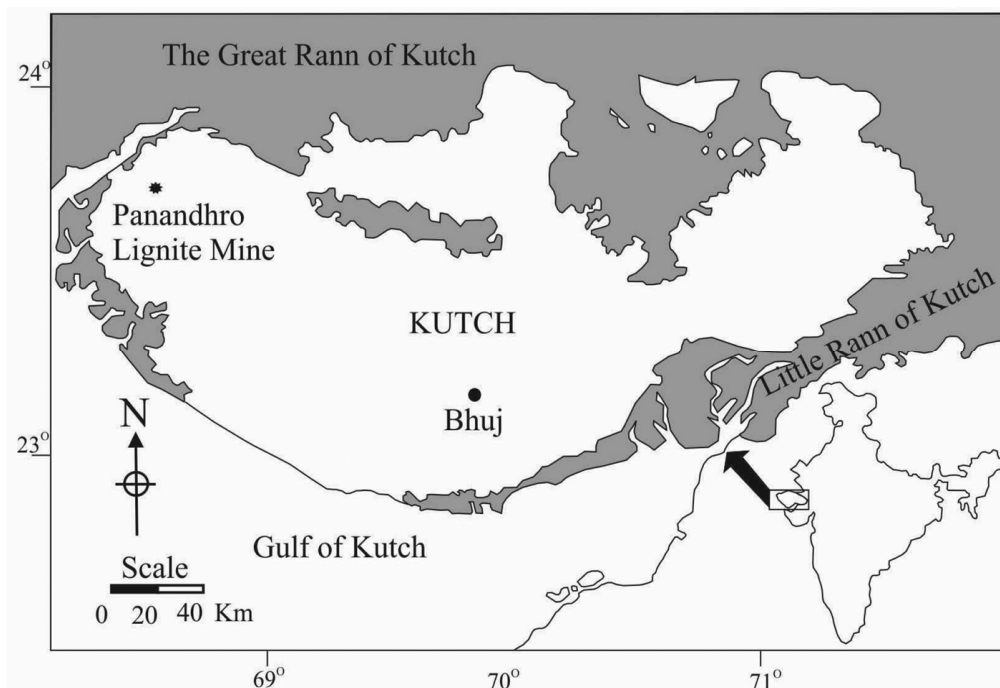*For correspondence. (e-mail: runciepaulmathews@gmail.com)

Figure 1. Location map of Panandhro lignite mine, Kachchh Basin, western India[36].

Age	Formation	Environment	Lithology
Plio-Pleistocene	Sandan	Littoral/Foreshore	
	····· Unconformity ·····		
Middle Miocene	Chhasra	Marine inner shelf	
Early Miocene	Khari Nadi	Marine foreshore	
	····· Unconformity ·····		
Oligocene	Maniyara Fort	Marine shelf	
	····· Unconformity ·····		
Middle Eocene to early late Eocene	Fulra limestone	Open marine carbonate platform	
Early middle Eocene	Harudi	Lagoonal to nearshore	
	····· Unconformity ·····		
Late Palaeocene to early Eocene	Naredi	Lagoonal	
	····· Unconformity ·····		
Early Palaeocene	Matanomadh	Terrestrial	
	····· Unconformity ·····		
Late Cretaceous to early Palaeocene	Deccan Trap	Terrestrial lava flow	

Figure 2. Generalized Cenozoic lithostratigraphic sequence of Kachchh Basin, western India[17].

10 sec. Conditions for the GC system were as follows: splitless injection onto a 50 m DB5 column with an initial oven temperature of 40°C held for 2 min, then heated with 4°C min^{-1} to 300°C. The oven was then maintained isothermally for 15 min. The inner diameter of the column was 250 μm and the film thickness was 0.25 μm. The carrier gas was helium. Mass spectrometric acquisition was conducted on a 5970 MSD system. Dwell times were 65 μs for the cycle time of ~1.4/s.

FTIR, a technique used to study emission or absorption of infrared radiation, is employed to identify various functional groups[18,21], chemical structure characterization of coal macerals[22–27] and kerogen in source rocks[28–30]. The spectrum obtained can give crucial information about the molecular structure of organic compounds, especially functionalities such as aromatic, aliphatic, carbonyl and hydroxyl groups. The FTIR spectrum of solid bitumen from the Panandhro lignite field is shown in Figure 3 a. The spectrum of the bitumen is characterized by a medium hydroxyl (OH) band in the region 3600–3100 cm^{-1}. A prominent aliphatic CH_x stretching band is present between 2940 and 2915 cm^{-1} and 2870–2850 cm^{-1}. Although present, the aromatic C=O stretching band is weak, whereas the aromatic C=C stretching band peaking at ~1622 cm^{-1} is relatively strong.

The aliphatic deformation/bending peak characterized at 1443 cm^{-1} showed absorption similar to that of the aromatic C=C band. All the oxygen containing compounds showed a medium intense absorption peaks. The deformation of CH_2 and CH_3 at 1368 cm^{-1} and 1314 cm^{-1} respectively, showed more intense absorption peaks than that of the aliphatic ethers and alcohols absorbed between 1100 cm^{-1} and 1000 cm^{-1}. The CH out-of-plane deformation also showed weak absorption between 900 cm^{-1} and

700 cm^{-1}. A comparison of Eocene Panandhro solid bitumen spectrum with that of the Miocene Neyveli solid bitumen showed similar characteristics (Figure 3 b), suggesting similar chemical composition and origin.

Several FTIR-derived indices or semi-quantitative ratios were used to characterize coal/lignite macerals[22–24,27,29]. These evaluations utilized the integrated peaks areas of major functional groups. The ratios can reveal the aromaticity (AR$_1$: aromatic stretching CH/aliphatic stretching CH), aliphatic chain length (ACL: CH$_2$/CH$_3$), A and C factors and petroleum potential (FA: CH$_2$ in aliphatic stretching/CH$_2$ in aliphatic stretching + aromatic carbon C=C). The AR$_1$ (3100–3000 cm^{-1}/2800–3000 cm^{-1}) values are negligible or absent in the solid bitumen (Table 1). In comparison with macerals, similar values were found in cutinite (cuticles) and alginite (algae) which are highly aliphatic[27]. This shows that solid bitumen is highly aliphatic in nature.

The CH$_2$/CH$_3$ (2940–2915 cm^{-1}/2975–2950 cm^{-1}) intensity ratio was used to calculate the length and degree of branching of aliphatic side chain. Study of macerals showed that the CH$_2$/CH$_3$ ratio is highest in alginite followed by cutinite, suggesting longest aliphatic side chains[20,27]. Other macerals of the liptinite group and vitrinite/huminite group consist of relatively shorter side chains. The ratios for Panandhro and Neyveli solid bi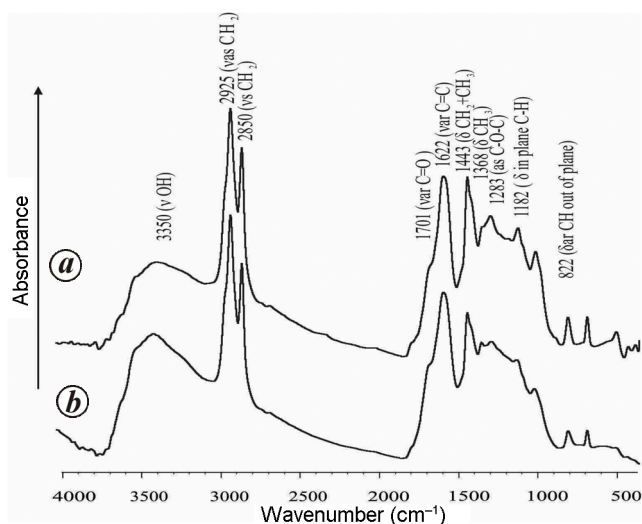tumens were 2.05 and 2.04 respectively. These values are comparable with values of resinite (resins/wax), sporinite (spores-pollen), bituminite and huminite, suggesting shorter chain length of aliphatic side chains in the solid bitumen.

The A factor ((3000–2800 cm^{-1}/3000–2800 cm^{-1}) + 1650–1520 cm^{-1}) which represents changes in the relative intensities of the aliphatic groups, and the C factor ((1800–1650 cm^{-1}/1820–1650 cm^{-1}) + 1650–1520 cm^{-1}) which represents the changes in the C=O groups is used to demonstrate the kerogen types and maturation[28,31]. Here instead of peak intensity, band area was used[20]. The A factor versus C factor plot indicates that the solid bitumens studied contain type-II kerogen/organic matter (Figure 4). FA is much higher in liptinite macerals than those of the huminite/vitrinite maceral group[26]. The solid bitumen showed FA value 0.29 which is comparable with the
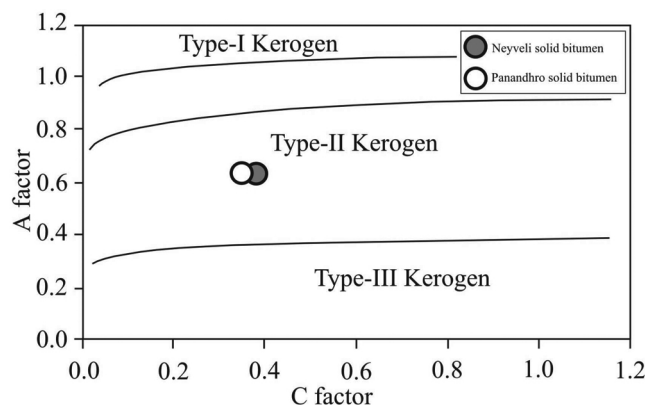

Figure 4. A factor versus C factor plot of Panandhro and Neyveli solid bitumen.

Figure 3. FTIR spectra of solid bitumen from (a) Panandhro lignite mine and (b) Neyveli lignite mine.

Table 1. FTIR semi-quantitative ratios for Panandhro and Neyveli solid bitumen

Sample	CH$_2$/CH$_3$	AR$_1$	FA	A factor	C factor
Panandhro solid bitumen	2.05	0.00	0.29	0.66	0.34
Neyveli solid bitumen	2.04	0.01	0.29	0.65	0.38

Table 2. Compounds identified in the pyrolysis mass chromatogram and their retention time

| Retention time (min.)	Compound	Molecular weight
5.39	C$_5$ n-alkane	72
7.94	C$_6$ n-alkane	86
9.17	Benzene	78
10.98	C$_7$ n-alkane	100
13.10	Toluene	92
14.35	C$_8$ n-alkane	114
17.08	Dimethyl benzene	106
18.30	C$_9$ n-alkane	128
20.85	C$_3$ benzene	120
22.35	C$_{10}$ n-alkane	142
23.35	C$_4$ alkyl benzene	134
26.34	C$_{11}$ n-alkane	156
30.13	C$_{12}$ n-alkane	170
33.74	C$_{13}$ n-alkane	184
37.13	C$_{14}$ n-alkane	198
40.36	C$_{15}$ n-alkane	212
43.22	C$_{16}$ n-alkane	226
46.07	C$_{17}$ n-alkane	240
48.72	C$_{18}$ n-alkane	254
51.32	C$_{19}$ n-alkane	268
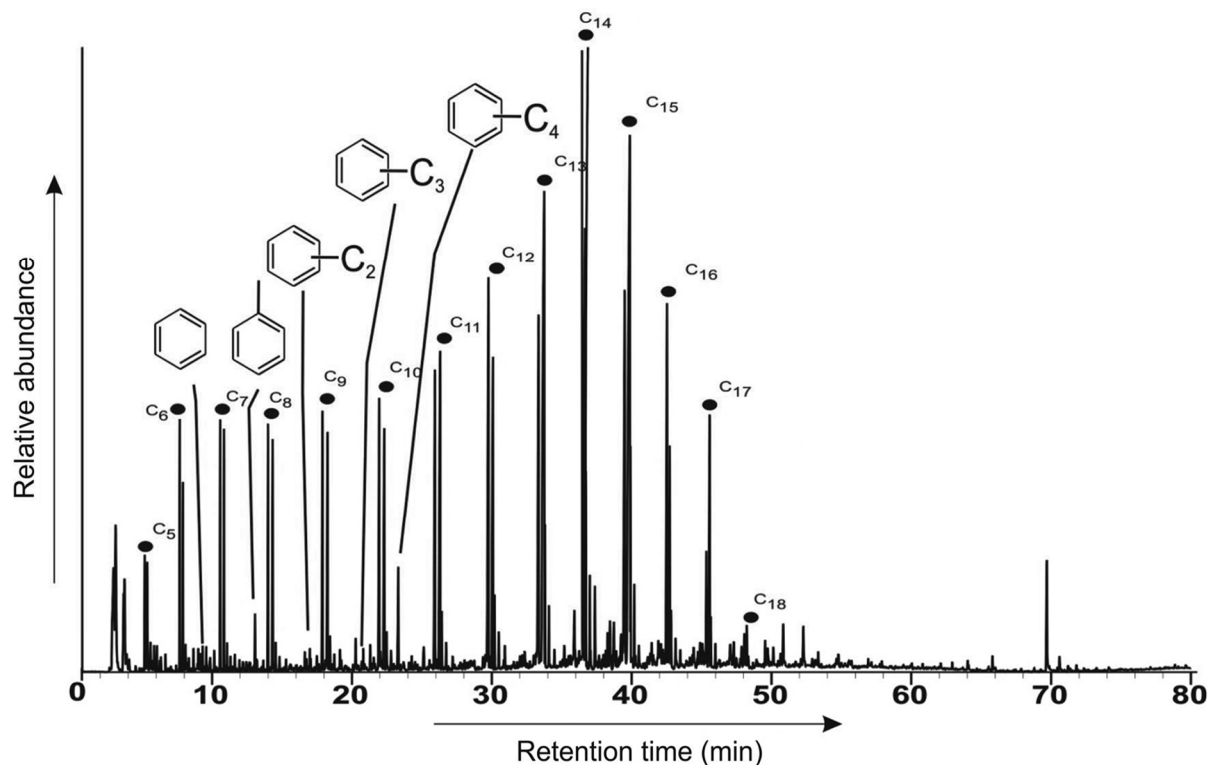
Figure 5. Pyrolysis mass chromatogram of Panandhro solid bitumen, Kachchh Basin (black dots indicating *n*-alkanes).

huminite macerals, which are of low oil potential. How-ever, an earlier study showed the importance of solid bitumen as a source of gas[32]. Our study also suggests that like huminite macerals, solid bitumen could also be a source of gaseous hydrocarbon.

The mass chromatogram of the analysed sample is presented in Figure 5. The identified compounds, their re-tention time and molecular weight are listed in Table 2. The chromatogram characterized by saturated compounds (nC_5 to nC_{18}) are easily discernable. Aromatic compounds such as benzene, toluene, C_3 and C_4 benzene are also found, but are relatively less abundant. Biomarker study established that the bitumen can be of pre-oil generation and post-generation types[2]. The pre-oil generation solid bitumens are viscous fluids extruded from their source rocks and migrated only a short distance. They are void or fracture fillings and are intimately associated with source rocks. They are more aliphatic. Post-generation types are produced by the alteration of already formed crude oils, generated and migrated long distances from a source rock and finally biodegraded. Thus, they are the residue of oil and are more aromatic[2,30].

The T_{max} values of the Panandhro lignites, determined through Rock-Eval pyrolysis[33], vary between 405°C and 429°C. Although the low T_{max} values indicate a low ther-mal maturity of lignites, higher values nearing 430°C indicate that some samples have almost reached the tem-perature required for hydrocarbon generation. The humi-nite reflectance values (0.35–0.44% R_o) also indicate that the Panandhro lignite belongs to a relatively higher rank[34,35], as compared to other lignites of western India, suggesting higher thermal maturity. This shows that certain amounts of bitumens were generated by the heat then trapped in the cracks/fissures of the lignites, and later got solidified; suggesting its pre-oil generation nature.

Our geochemical study reveals that the Panandhro lignites appear to have crossed the minimum temperature required for the generation and expulsion of bitumen. Subsequently filled and solidified in the cracks and pores of the lignite itself, the solid bitumen is characterized by its highly aliphatic nature, and pre-oil generation source. Although the kerogen (organic matter) is of type-II, the relatively low FA indicates its low oil source potential. However, the presence of solid bitumen in the studied lignite bearing sequence can definitely contribute to the generation of gaseous hydrocarbon.

1. Tissot, B. and Welte, D. H., *Petroleum Formation and Occur-rence*, Springer, Berlin, 1984, 2nd edn, p. 699.
2. Curiale, J. A., Origin of solid bitumens, with emphasis on biological marker results. *Org. Geochem.*, 1986, **10**, 559–580.
3. Kelemen, S. R. *et al.*, Distinguishing solid bitumens formed by thermochemical sulfate reduction and thermal chemical alteration. *Org. Geochem.*, 2008, **39**, 1137–1143.
4. Patel, P. D., Christman, P. G. and Gardner, J. W., Investigation of unexpectedly low field-observed fluid mobilities during some CO_2 tertiary floods. *SPE Reservoir Eng.*, 1987, 507–513.

5. Lomando, A. J., The influence of solid reservoir bitumen on reservoir quality. *AAPG Bull.*, 1992, **76**, 1137–1152.

6. Jacob, H., Classification, structure, genesis and practical importance of natural solid oil bitumen ('migrabitumen'). *Int. J. Coal Geol.*, 1989, **11**, 65–79.

7. Gentzis, T. and Goodarzi, F., A review of the use of bitumen reflectance in hydrocarbon exploration with examples from Melville Island, Arctic Canada. In *Applications of Thermal Maturity Studies to Energy Exploration* (eds Nuccio, V. F. and Barker, C. E.), SEPM Special Publications, 1990, pp. 23–36.

8. Landis, C. R. and Castaño, J. R., Maturation and bulk chemical properties of a suite of solid hydrocarbons. *Org. Geochem.*, 1995, **22**, 137–149.

9. Abraham, H., *Asphalts and Allied Substances*, Van Nostrand, New York, 1960, vol. 5, p. 133.

10. Walters, C. C., Kelemen, S. R., Kwiatek, P. J., Pottorf, R. J., Mankiewicz, P. J., Curry, D. J. and Putney, K., Reactive polar precipitation via ethercross-linkage: a new mechanism for solid bitumen formation. *Org. Geochem.*, 2006, **37**, 408–427.

11. Gonçalves, P. A., Mendonça Filho, J. G., da Silva, F. S. and Flores, D., Reprint of 'Solid bitumen occurrences in the Arruda sub-basin (Lusitanian Basin, Portugal): Petrographic features'. *Int. J. Coal Geol.*, 2015, **139**, 217–227.

12. Fink, R., Virgo, S., Arndt, M., Visser, W., Littke, R. and Urai, J. L., Solid bitumen in calcite veins from the Natih Formation in the Oman Mountains: Multiple phases of petroleum migration in a changing stress field. *Int. J. Coal Geol.*, 2016, **157**, 39–51.

13. Raju, S. V. and Mathur, N., Rajasthan lignite as a source of unconventional oil. *Curr. Sci.*, 2013, **104**, 752–757.

14. Singh, A. and Singh, B. D., Progenitors of hydrocarbon in Indian coals and lignites and their significance. *Mem. Geol. Soc. India*, 2008, **71**, 117–133.

15. Dwivedi, A. K., Petroleum exploration in India – A perspective and endeavours. *Proc. Indian Natl. Sci. Acad.*, 2016, **82**(3), 881–903.

16. Biswas, S. K.., Status of petroleum exploration in India. *Proc. Indian Natl. Sci. Acad*, 2012, **78**(3), 475–494.

17. Biswas, S. K., Tertiary stratigraphy of Kutch. *J. Palaeontol. Soc. India*, 1992, **37**, 1–29.

18. Painter, P. C., Snyder, R. W., Starsinic, M., Coleman, M. M., Kuehn, D. W. and Davis, A., Concerning the applications of FTIR to the study of coal: a critical assessment of band assignments and the application of spectral analysis programs. *Appl. Spectrosc.*, 1981, **35**, 475–485.

19. Painter, P. C., Starsinic, M. and Coleman, M. M., Determination of functional groups in coal by fourier transform interferometry. In *Fourier Transform Infrared Spectrometry* (eds Ferraro, J. R. and Basile, L. J.), Academic Press, New York, 1985, pp. 169–240.

20. Guo, Y. and Bustin, R. M., Micro-FTIR spectroscopy of liptinite macerals in coal. *Int. J. Coal Geol.*, 1997, **36**, 259–275.

21. Chen, Y., Furmann, A., Mastalerz, M. and Schimmelmann, A., Quantitative analysis of shales by KBr-FTIR and micro-FTIR. *Fuel*, 2014, **116**, 538–549.

22. Chen, Y., Mastalerz, M. and Schimmelmann, A., Characterization of chemical functional groups in macerals across different coal ranks via micro-FTIR spectroscopy. *Int. J. Coal Geol.*, 2012, **104**, 22–33.

23. Mastalerz, M. and Bustin, R. M., Variation in macerals chemistry within and between coals of varying rank: An electron microprobe and micro-Fourier transform infrared investigation. *J. Microsc.*, 1993, **171**, 153–166.

24. Lyons, P. C., Orem, W. H., Mastalerz, M., Zodrow, E. L., Redemann, A. V. and Bustin, R. M., C-NMR, micro-FTIR and fluorescence spectra, and pyrolysis-gas chromatograms of coalified foliage of Late carboniferous medullosan seed ferns, Nova Scotia, Canada: implications for coalification and chemotaxonomy. *Int. J. Coal Geol.*, 1995, **27**, 227–258.

25. Guo, Y., Renton, J. J. and Penn, J. H., FTIR micro-spectroscopy of particular liptinite-(lopinite) rich, Late Permian coals from Southern China. *Int. J. Coal Geol.*, 1996, **29**, 187–196.

26. Ibarra, J. V., Munoz, E. and Moliner, R., FTIR study of the evolution of coal structure during the coalification process. *Org. Geochem.*, 1996, **24**, 725–735.

27. Mastalerz, M., Hower, J. C. and Taulbee, D. N., Variations in chemistry of macerals as reflected by micro-scale analysis of a Spanish coal. *Geologica Acta*, 2013, **11**, 483–493.

28. Ganz, H. and Kalkreuth, W., Application of the infrared spectroscopy to the classification of kerogen-types and the evolution of source rock and oil shale potentials. *Fuel*, 1987, **66**, 708–711.

29. Kister, J., Guiliano, J. M., Largeau, C., Derenne, S. and Casadevall, E., Characterization of chemical structure, degree of maturation and oil potential torbanates (type I Kerogen) by quantitative FTIR spectroscopy. *Fuel*, 1990, **69**, 1357–1361.

30. Lin, R. and Ritz, P., Studying individual macerals using IR micro-spectroscopy and implication on oil versus gas/condense proneness and 'low-rank' generation. *Org. Geochem.*, 1993, **20**, 695–706.

31. Mastalerz, M. and Glikson, M., *In-situ* analysis of solid bitumen in coal: examples from the Bowen basin and the Illinois Basin. *Int. J. Coal. Geol.*, 2000, **42**, 207–220.

32. Glikson, M., Boreham, C. J. and Thiede, D. S., Coal composition and mode of maturation, a determining factor in quantifying hydrocarbon species generated. In *Coalbed Methane: Scientific and Economic Evaluation* (eds Mastalerz, M., Glikson, M. and Golding, S.), Kluwer, Dordrecht, 1991, vol. 33, pp. 155–185.

33. Sahay, V. K., The hydrocarbon potential, thermal maturity, sequence stratigraphic setting and depositional palaeoenvironment of carbonaceous shale and lignite successions of Panandhro, northwestern Kutch Basin, Gujarat, Western India. *Central Eur. J. Geosci.*, 2011, **3**, 12–28.

34. Singh, A., Rank assessment of Panandhro lignite deposit, Kutch Basin, Gujarat. *J. Geol. Soc. India*, 2002, **59**, 69–77.

35. Singh, A. and Singh, B. D., Petrology of Panandhro lignite deposit, Gujarat in relation to palaeodepositional condition. *J. Geol. Soc. India*, 2005, **66**, 334–344.

36. Sharma, J. and Saraswati, P. K., Lignites of Kutch, Western India: Dinoflagellate biostratigraphy and palaeoclimate. *Rev. Micropalaeontol.*, 2015, **58**, 107–119.